Evaluation of the Impact of Pigpen Type on Airflow and Temperature Field in Closed Piggeries Using CFD

Chengguo Fu, Yuhao Li, Weiwei He, Ting Chen, Hui Yang, Haibo Li, Yaqi Zhang, Hongbin Cong

***Abstract*—Ventilation serves as the primary method for regulating the environment within a piggery, and the design of various pigpens can significantly influence airflow patterns. To explore the influence on airflow trajectory, computational fluid dynamics (CFD) was used to simulate airflow and temperature in piggeries with four pigpen types: TA (solid boards), TB (upper fence and lower solid board), TC (solid boards and fences), and TD (fence structures). Results showed:(1) TB enabled manure pit airflow to enter the pig activity area more easily. (2) TA was prone to cyclone formation with reverse airflow, while TB had fewer. TC's aisle fence enhanced enclosure ventilation, yet the pigs' breathing plane mainly had reverse airflow, and TD had positive airflow. (3) Different plans had varying wind speeds and temperatures at pigs' breathing height. TC had the lowest average breathing plane temperature and relatively low wind speed, providing effective cooling and low wind speed. Its temperature variation coefficient (2.71%) was lower than others, facilitating better temperature control. This study on pigs' breathing zone conditions in four pigpen types offers references and theoretical insights for future piggery construction.**

***Index Terms*—CFD, numerical simulation, piggery, pigpen, temperature, ventilation**

I. Introduction

THE environmental quality of piggeries is a crucial factor influencing the healthy growth of pigs, with ventilation serving as the primary method for regulating this quality [1-5]. In the existing research on ventilation in piggeries, scholars mainly concentrate on the position and area of ventilation openings, often neglecting the impact of pigpen type on ventilation [6-9]. Pigpens is the smallest unit in the piggery and play a significant role in determining airflow and temperature. Therefore, it is essential to explore the relationship between pigpen type and the environmental conditions, thereby establishing a scientific foundation for future piggery construction.

Currently, the planar structure of closed piggeries is predominantly rectangular, with longitudinal mechanical ventilation being the preponderant method utilized. Under fixed ventilation circumstances and construction patterns, the type of pigpen frequently represents a crucial factor influencing the environmental conditions within the pig activity areas. Based on the survey, there are primarily two pigpen categories: solid boards and fences. Enclosures constructed with solid boards can effectively segregate airflow between adjacent enclosures, which is beneficial for epidemic prevention. However, such a design is disadvantageous to ventilation and management. Conversely, enclosures constructed with fences afford favorable ventilation and convenient management, but excessive airflow might engender discomfort and energy dissipation for the pigs. To explore the impacts of different types of pigpens on ventilation and temperature in pig activity areas, this study intends to employ computational fluid dynamics (CFD) technology to analyze the environmental changes within the pigpens [10-13].

CFD technology has a broad range of applications, such as the simulation of ventilation, temperature variations, and pollutant volatilization within livestock housing [11, 13 - 16]. Wei, X. et al. [17] utilized CFD technology to simulate the changes and distribution of temperature and airflow in pigsties, reporting a temperature difference between the simulated temperature and the actual temperature was less than 1.54°C. Mossad, R. R. [18] analyzed the impact of the number and position of ventilation openings on airflow and temperature using CFD technology, ultimately determining the optimal solution. Yang, H. et al. [19] simulated and analyzed airflow, temperature, humidity, and NH_3 concentration in a closed piggery. By identifying the environmental characteristic points, and then subsequently planning the inspection path and monitoring points for the track inspection robot, can substantially enhance the scientific and rational arrangement of monitoring points. La, A. et al. [20] established a CFD model to simulate the

Manuscript received August 24, 2024; revised January 15, 2025. This work was supported in part by Joint Funds of the National Natural Science Foundation of China (52301205), and Henan Province Science and Technology Research and Development Projects (242102320150).

Chengguo Fu is an associate professor of the School of Mechanical Engineering, Guizhou University of Engineering Science, China (Corresponding author; E-mail: scu_fcg@163.com).

Yuhao Li is a PhD candidate of the College of Engineering, South China Agricultural University, China (Co-first author; E-mail: lyvhao@163.com).

Weiwei He is a postgraduate Student of the School of Mechanical and Electrical Engineering, Henan Institute of Science and Technology, China (E-mail: wei989926@163.com).

Ting Chen is a postgraduate Student of the School of Mechanical and Electrical Engineering, Henan Institute of Science and Technology, China (E-mail: chenting_future@163.com).

Hui Yang is an experimentalist of the School of Mechanical and Electrical Engineering, Henan Institute of Science and Technology, China (E-mail: abcyah@163.com).

Haibo Li is a lecturer of the School of Mechanical and Electrical Engineering, Henan Institute of Science and Technology, China (E-mail: skyseal@126.com).

Yaqi Zhang is an associate professor of the School of Mechanical and Electrical Engineering, Henan Institute of Science and Technology, China (E-mail: zhangyaqi_1988@163.com).

Hongbin Cong is a researcher of the Academy of Agricultural Planning and Engineering, Ministry of Agriculture and Rural Affairs, China (E-mail: dabinc123@163.com).

propagation and distribution of the porcine reproductive and respiratory syndrome virus in piggery environments. Tabase, P. K. et al. [21] applied CFD technology to analyze the effects of under-floor ventilation systems on airflow and ammonia (NH_3) distribution in piggery settings. Based on current research data, several schemes can be proposed for simulating the environmental conditions of animal husbandry facilities. The solver type is typically selected as pressure-based [21]; the viscous model generally adopts the Standard k-ε model [22-25]; the solution method employed is SIMPLE (semi-implicit method for pressure linked equations) [24, 26]; for the spatial discretization format, the pressure term is set to second order; under complex flow conditions, the second order upwind scheme is preferred for the discretization of momentum, turbulent kinetic energy, turbulent dissipation rate, and energy to enhance computational accuracy [21, 24, 26, 27]. Currently, in CFD simulations, the relative error of temperature can be maintained below 10% [28, 29]. Evidence indicates that the wind speed error at most monitoring points can be kept below 30% during the research process, with the minimum error reaching within 5% [24, 29-31]. Therefore, it can be concluded that a judicious selection of computational models and modeling methods is essential for minimizing simulation errors [32, 33].

In summary, to strengthen the analysis of environmental changes inside the piggery and provide a scientific basis for the construction of future piggery facilities, it is of utmost importance to explore the types of pigpens as well as the airflow dynamics therein. The application of CFD technology to study the distribution of environmental factors, such as airflow fields and temperature fields, within piggeries can significantly economize scientific research resources. In this context, the present study focuses on closed nursery piggeries as the research object and utilizes computational models to simulate the impacts of diverse types of pigpens on wind speed and temperature. By analyzing the characteristics of changes in wind speed and temperature, this research endeavors to identify the environmental influences associated with different pigpen designs, thereby improving the environmental quality of pig facilities, reducing energy consumption, and augmenting the production efficiency of pig farming.

II. Materials and Methods

A. Structure of Piggery

This study focuses on the traditional closed nursery piggery located in the Henan province, with the structure and ventilation system layout illustrated in Fig. 1. In this layout, the positive *y*-axis direction is oriented to the right side of the piggery, where the pigpen numbers range from No.1 to No.10. Conversely, the negative *y*-axis direction points to the left, covering pigpen numbers No.11 to No.20. The positive *x*-axis direction extends toward the rear of the piggery, while the negative *x*-axis direction is directed toward the front. Additionally, the positive *z*-axis direction points to the top of the piggery, with the negative *z*-axis direction points towards the bottom of the manure pit. The pigpens are symmetrically arranged on both sides, with ten pigpens on each side, each having dimensions of 4.5 × 4 × 1 m. The piggery adopts a negative-pressure mechanical ventilation system, with a wet curtain on the front wall as the air inlet and a fan on the back wall as the air outlet. The dimensions of the wet curtain are 4 × 1.7 m, while the fans measure 1.5 × 1.5 m, 1.1 × 1.1 m, and 0.8 × 0.8 m. The facility accommodates approximately 360 nursery pigs. The manure pit has a depth of 1.2 m, and airflow exchange with the pig activity area occurs solely through the slatted floor, with no vents located elsewhere. A 0.5 m wide aisle is located between the front and rear walls and the adjacent pigpens.

B. Types of Pigpens

In piggeries, four common types of pigpens can be identified: pigpens constructed with solid boards (TA), pigpens constructed with a combination of semi-solid boards and semi-fences (TB), hybrid pigpens (TC), and pigpens

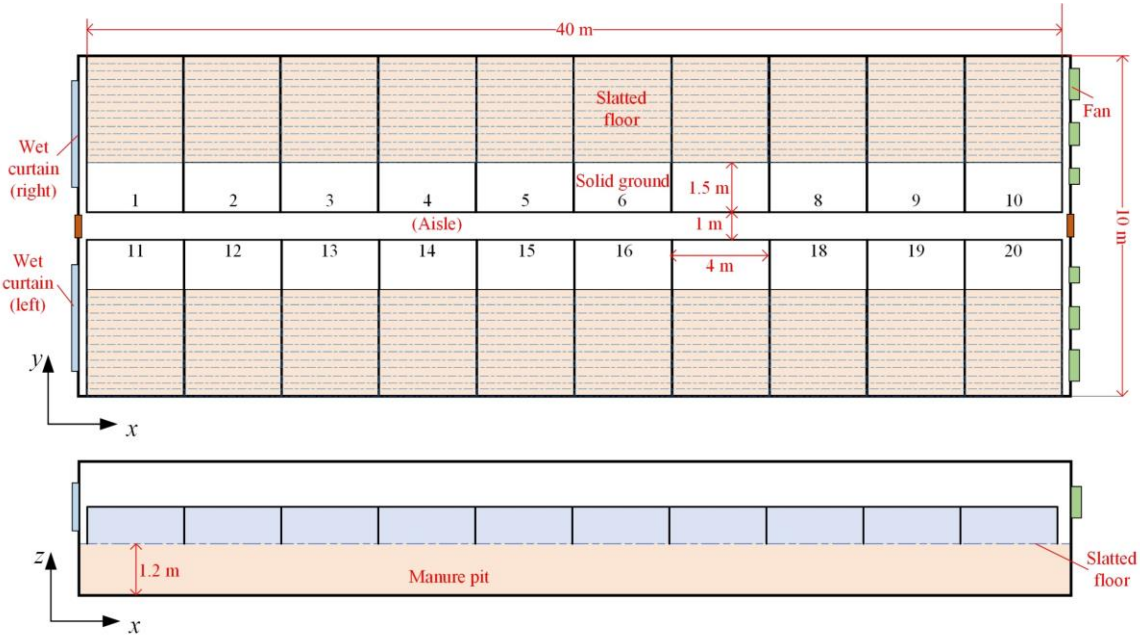

Fig. 1. The structure of the piggery and the layout of the pigpens.

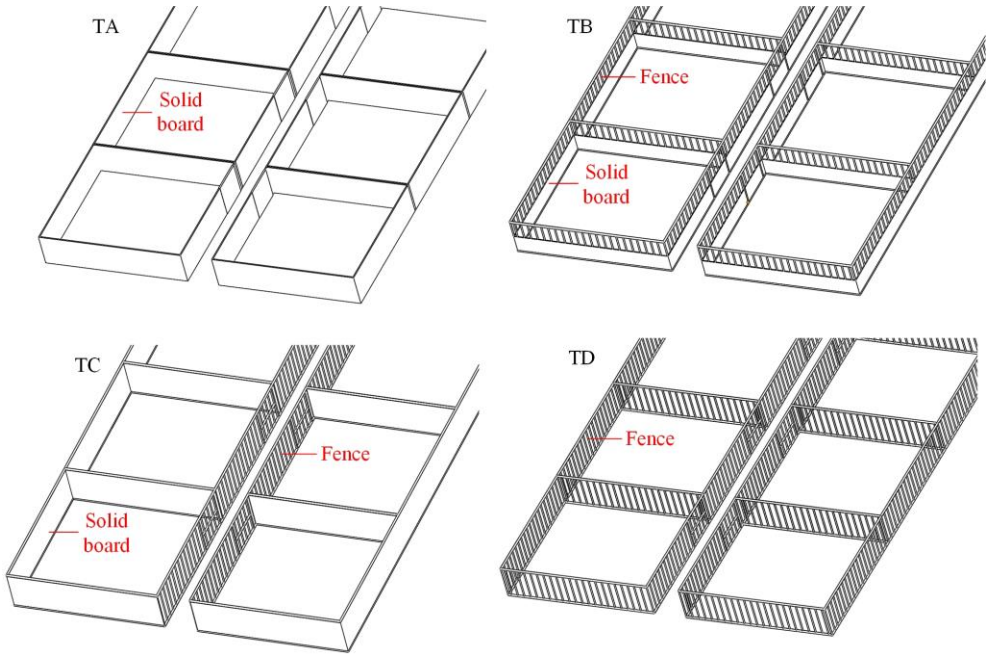

Fig. 2. Types of pigpens.

constructed solely with fences (TD). The detailed structure of the pigsty is shown in Fig. 2. The TA pigpen is constructed from solid boards and has a height of 1 m, which effectively blocks airflow parallel to the ground. In contrast, the TB features a lower section composed of solid boards with a height of 0.5 m, and it is topped with a fence of the same height. The TC pigpen consists of solid boards with a height of 1 m on three sides, while the side adjacent to the aisle is constructed using a fence. Finally, the TD pigpen is entirely made up of a fence and has a height of 1 m.

C. Methods and Steps

In this study, CFD technology was employed to simulate the environment of a piggery. Utilizing the simulation data, the influence of different types of pigpens on the wind speed trajectory and temperature within the piggery was analyzed. The detailed research steps are as follows:

(1) Construction of structural model

Analyze the structural architecture of the piggery, measure its dimensional parameters, and utilize CFD technology to construct a structural model. Refer to simulation cases to ascertain a simplified model for complex structures, thereby enhancing computational efficiency and reducing simulation errors.

(2) Determination of research area

In this study, the nursery piggery was selected as the research object, with the respiratory height of the nursery pigs serving as the focal area of investigation. By consulting relevant literatures and actual conditions, the respiratory height of the nursery pigs was set at 0.4 m.

(3) Division of monitoring points

To facilitate a more effective comparison of the disparities among diverse monitoring points, this study established environmental monitoring points with pigpens as basic unit. Each pigpen is furnished with 13 monitoring points, thereby yielding a cumulative total of 260 monitoring points throughout the entire piggery. The detailed information regarding the monitoring points is presented in Fig. 3.

(4) Acquisition of environmental data

Using environmental monitoring equipment to gather environmental parameters inside the piggery, and set boundary conditions for the simulation model.

(5) Calculation and analysis of results

Firstly, a comprehensive analysis of the literature and relevant simulation cases was conducted to determine the optimal computational model. Secondly, under identical environmental conditions, only the type of pigpen was altered, and ANSYS (Version 14.5) software was employed for simulation calculations to obtain wind speed and temperature variations within the piggery. Finally, based on the simulation data, a comparison and analysis are conducted to assess the impact of different types of pigpens on the environmental conditions of the pig activity areas.

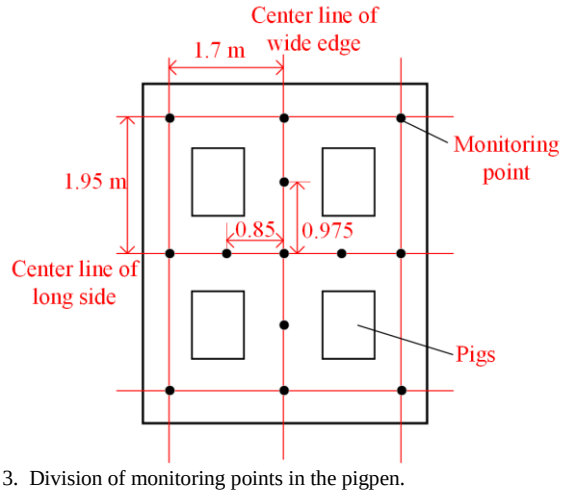

Fig. 3. Division of monitoring points in the pigpen.

D. CFD Simulation

Construction of Structural Model and Grid Division

A three-dimensional structural model of a piggery was established by ANSYS software. Each pigpen accommodates approximately 18 to 20 pigs. To improve computational efficiency, the pigs within each pigpen were simplified and represented by four cubes, with each cube having dimensions

of 0.7 × 0.25 × 0.5 m [34]. Factors such as crossbeams, feeders, water pipes, and other elements that exert a relatively insignificant influence on the simulation results were excluded from the model. Following a grid independence verification, the piggery was segmented into a total of 2,945,258 grids.

Basic Control Equations

During the simulation process, the air inside the piggery is set as an incompressible fluid, following the laws of conservation of mass (equation 1), momentum (equation 2), and energy (equation 3).

Conservation of mass equation:

$$\frac{\partial(\rho u)}{\partial x}+\frac{\partial(\rho v)}{\partial y}+\frac{\partial(\rho w)}{\partial z}=0 \tag{1}$$

ρ represents the density of fluid in the pigsty, kg·m^{-3}; u, v, and w respectively denote the components of fluid velocity in the x, y, and z directions of the coordinate axis, m·s^{-1}.

Momentum conservation equation:

$$\begin{cases}\dfrac{\partial(\rho uu)}{\partial x}+\dfrac{\partial(\rho uv)}{\partial y}+\dfrac{\partial(\rho uw)}{\partial z}= \\ \dfrac{\partial}{\partial x}\left(\mu\dfrac{\partial u}{\partial x}\right)+\dfrac{\partial}{\partial y}\left(\mu\dfrac{\partial u}{\partial y}\right)+\dfrac{\partial}{\partial z}\left(\mu\dfrac{\partial u}{\partial z}\right)-\dfrac{\partial p}{\partial x} \\ \dfrac{\partial(\rho vu)}{\partial x}+\dfrac{\partial(\rho vv)}{\partial y}+\dfrac{\partial(\rho vw)}{\partial z}= \\ \dfrac{\partial}{\partial x}\left(\mu\dfrac{\partial v}{\partial x}\right)+\dfrac{\partial}{\partial y}\left(\mu\dfrac{\partial v}{\partial y}\right)+\dfrac{\partial}{\partial z}\left(\mu\dfrac{\partial v}{\partial z}\right)-\dfrac{\partial p}{\partial y} \\ \dfrac{\partial(\rho wu)}{\partial x}+\dfrac{\partial(\rho wv)}{\partial y}+\dfrac{\partial(\rho ww)}{\partial z}= \\ \dfrac{\partial}{\partial x}\left(\mu\dfrac{\partial w}{\partial x}\right)+\dfrac{\partial}{\partial y}\left(\mu\dfrac{\partial w}{\partial y}\right)+\dfrac{\partial}{\partial z}\left(\mu\dfrac{\partial w}{\partial z}\right)-\dfrac{\partial p}{\partial z}-\rho g\end{cases} \tag{2}$$

μ represents the dynamic viscosity coefficient, pa·s; p represents the pressure on the fluid, Pa.

Energy conservation equation:

$$\begin{aligned}&\frac{\partial(\rho uT)}{\partial x}+\frac{\partial(\rho vT)}{\partial y}+\frac{\partial(\rho wT)}{\partial z}= \\ &\frac{\partial}{\partial x}\left(\frac{k}{c_p}\frac{\partial T}{\partial x}\right)+\frac{\partial}{\partial x}\left(\frac{k}{c_p}\frac{\partial T}{\partial y}\right)+\frac{\partial}{\partial x}\left(\frac{k}{c_p}\frac{\partial T}{\partial z}\right)+S_T\end{aligned} \tag{3}$$

T represents the temperature of the fluid inside the piggery, K; k represents the thermal conductivity of the fluid, W·(m·K)$^{-1}$; c_p represents the specific heat capacity of a fluid, J·(kg·K)$^{-1}$; S_T represents the heat source inside the fluid, W.

Simulation Calculation

The Ansys Fluent module calculated the temperature and wind speed within the piggery. The boundary conditions for the simulation are obtained from environmental data collected in a prior project [19]. The temperature settings were as follows: the right wall was set at 23 °C, the left wall at 22.1 °C, the front wall at 23.8 °C, the rear wall at 21.1 °C, the roof at 24.9 °C, the ground at 23.5 °C, and the surface temperature of the pig body at 38.2 °C. The wet curtain is designated as the pressure inlet, the fan serves as the speed outlet (Fans with dimensions of 1.5 × 1.5 m and 0.8 × 0.8 m, with a wind speed of 1.5 m·s^{-1}; a fan with a size of 1.1 × 1.1 m, a wind speed of m·s^{-1}). The temperature of the pigpen board was set to 24°C. The coupling effects among environmental factors were neglected, with the focus solely placed on the impact of longitudinal ventilation on the piggery. Additionally, the slatted floor is simplified as a porous medium model [10, 35-37].

The Solver Type was selected as pressure-based. The Standard k-ε model was adopted for the Viscosity Model, and the SIMPLE method was employed for the solution [24, 26]. For the spatial discretization scheme, the pressure term was discretized using a second-order scheme, the second-order upwind scheme was utilized for the discretization of momentum, turbulent kinetic energy, turbulent dissipation rate, and energy. The iterative calculation was considered to have converged when the residuals of the energy equation and other equations reach values of 10^{-6} and 10^{-3}, respectively, and when the environmental parameters at the monitoring points remain constant [38].

III. Results and Discussion

A. Analysis of Airflow Trajectory on xz Plane

Ventilation plays a crucial role in regulating the environmental quality of closed piggeries and exerts a significant impact on the overall piggery environment. The trajectory of airflow is of fundamental importance in dictating the distribution of diverse environmental factors. Hence, the wind speed field under different ventilation schemes is examined as a preliminary step. The principal aim of analyzing the airflow trajectory on the *xz* surface of the piggery is to explore the interrelationship among the upper airflow (the airflow above the pigpen), the airflow within the pigpen, and the airflow in the manure pit. Given the symmetrical structure of the piggery, one side (pigpens No.1-No.10) was chosen for this study. To mitigate the influence of the pig model, the *xz* plane was selected at a distance of 2 m from the right wall of the piggery. Moreover, the *xy* plane was selected at a height of 0.4 m above the ground to investigate the airflow trajectory at the breathing level of the pigs.

Analysis of Airflow Trajectory in TA Pigpen

The TA pigpen is constructed entirely from solid boards, which effectively obstruct airflow parallel to the ground, thereby protecting the pigs from its adverse effects. The trajectory of airflow in the *xz* plane is illustrated in Fig. 4. The upper airflow is minimally affected by obstacles, resulting in a relatively fast flow speed that is predominantly characterized by positive airflow (in the positive direction of the *x*-axis). In contrast, the airflow within the pigpen is influenced by the solid boards, leading to a more complex airflow trajectory. Additionally, the cesspool is connected to the pigpen through a slatted floor, causing its airflow path is affected by the airflow in the pigpen. The manure pit can be categorized into three regions based on the direction of airflow. The horizontal distance from the front wall to position MP1 (the boundary position of airflow) is 2 m, with the airflow moving in a positive direction. Concurrently, a cyclone will form at TA1 (the center of the cyclone is situated 0.4 m above the ground and 1 m from the front wall),

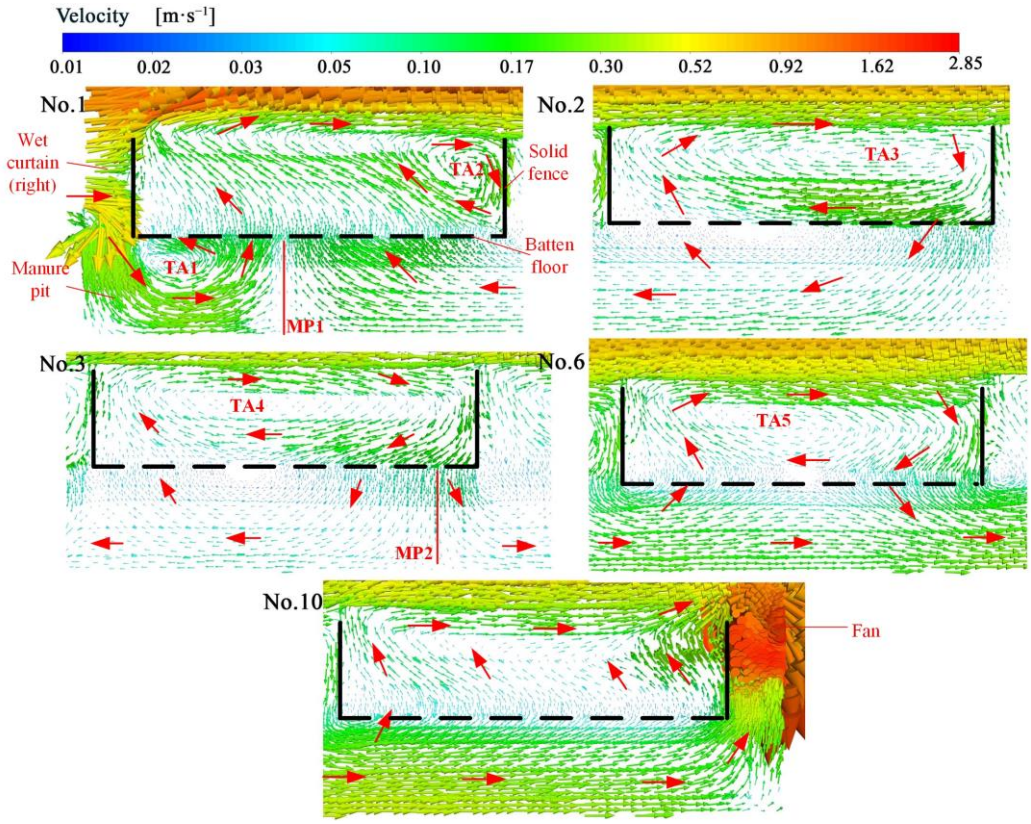

Fig. 4. Airflow trajectory on the *xz* surface of TA-type pigpen.

enabling the airflow to ultimately enter the No.1 pigpen through the slatted floor. The horizontal distance between positions MP1 and MP2 is 10 m, during which the airflow direction is reversed (in the negative *x*-axis direction). Furthermore, the horizontal distance from position MP2 to the back wall of the piggery is 28 m, where the airflow is again positive and exits the piggery through the fans.

Upon ingress from the wet curtain, the airflow is obstructed by a solid board located at the front of the pigpen. A portion of the airflow is directed into the manure pit via the slatted floor, while the remaining air enters the upper layer of the piggery and the interior of the pigpen. The comparative analysis is presented as follows:

(1) The Fig. 4 and Fig. 5 indicates that the mass flow rate of the airflow at the slatted floor in pigpen No.1 is 0.782 kg·s^{-1} (when the mass flow rate is positive, the airflow direction is positive along the *z*-axis; otherwise, it is negative.), with the airflow originating from both sides of MP1. After passing through the slatted floor, the upper airflow converges to form a cyclone parallel to the ground at TA2 (where the center of the cyclone is 0.6 m above the ground and 3.5 m away from the front solid board of the pigpen), which is located at the rear of pigpen No.1. Within the manure pit, a reverse airflow exists between positions MP1 and MP2, which drives the airflow in the manure pit toward the front of the piggery, thereby impeding improvements in air quality.

(2) The mass flow rates of the airflow at the slatted floor in pigpens No.2 and No.3 are –0.131 kg·s^{-1} and –0.234 kg·s^{-1}, respectively. The downward airflow partially moves toward the front of the pigpen and enters pigpen No.1 through the slatted floor. Meanwhile, another portion of the airflow recirculates back into the respective pigpen through the slatted floor at the front of each pigpen. A cyclone is present at TA3 in pigpen No.2, positioned 0.8 m above the ground and 2.5 m away from the solid board in front of the pigpen. Additionally, a cyclone is located at TA4 in pigpen No.3, situated 0.7 m above the ground and 1.5 m away from the solid board in front of the pigpen. In pigpen No.3, the airflow enters the manure pit and subsequently flows towards both sides at position MP2. Between position MP2 and the rear wall, the airflow is characterized being in the positive direction.

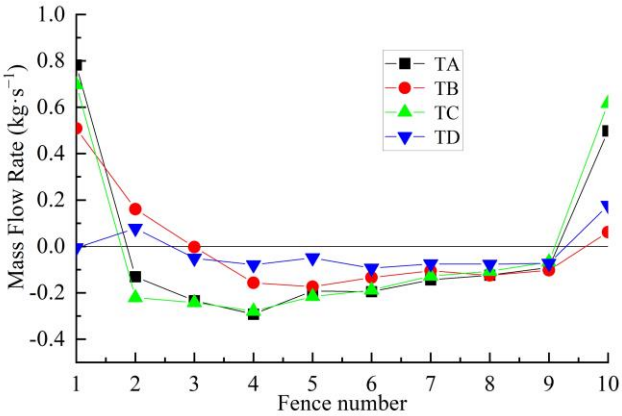

Fig. 5. Mass flow rate of airflow at the slatted floor in the pigpen.

(3) The airflow patterns within pigpens No.4 to No.9 are consistent with this observation. Specifically, the airflow enters the manure pit through the slatted floor located at the rear of the pigpen; a portion of this airflow disperses into the adjacent pigpens, while the remaining portion continues toward the rear of the pigpen, ultimately being discharged through fans. A cyclone is positioned at TA5 in pigpens No.4

- No.9, situated 0.4 m above the ground and 2 m away from the solid board in front of the pigpen.

(4) Pigpen No.10 is located near the fan at the end of the piggery. It is worthy of note that no cyclone exists inside this pigpen. The mass flow rate of airflow at the slatted floor is measured at 0.498 kg·s^{-1}. In pigpens No.1 and No.10, the predominant airflow is characterized by updrafts, whereas pigpens No.2 to No.9 exhibit downdrafts as the main airflow pattern.

Analysis of Airflow Trajectory in TB Pigpen

The upper section of the TB pigpen consists of a fence, while the lower section features a solid board, with the airflow within the pigpen being primarily influenced by the solid board. The airflow trajectory on the *xz* surface of the TB pigpen is illustrated in Fig. 6. In comparison to the TA pigpen, the TB pigpen enhances the ventilation efficiency within the pigpen. Additionally, the effect of the TB pigpen on the airflow inside the manure pit is comparable to that of the TA pigpen. The horizontal distance from the front wall of the piggery to position MP3 is 3 m, which is 50% longer than the TA scheme. Within this distance range, a cyclone exists at TB1, which is located at the same position as TA1. The horizontal distance between MP3 and MP4 is 20.3 m, which is 103% longer than the TA scheme. The distance between MP4 and the front wall of the piggery is 23.3 m, which is 94.17% longer than the TA scheme. The airflow between position MP4 and the front wall of the piggery will re-enter the pig activity area, which is detrimental to the healthy growth of pigs.

The height of the solid board of the TB pigpen is 0.5 m, which minimally obstructs the airflow. This low solid board prevents the formation of a cyclone in pigpen No.1, thereby reducing the harmful gas accumulation. The airflow between MP3 and MP4 flows in reverse, primarily influencing the airflow within pigpens No.1 to No.6. The comparative analysis is as follows:

(1) The mass flow rate of airflow at the slatted floor in pigpen No.1 is 0.509 kg·s^{-1}, which represents a decrease of 34.91% compared to the TA scheme.

(2) In pigpen No.2, the airflow predominantly originates from beneath the slatted floor at the front of the pigpen. The mass flow rate of this airflow is 0.161 kg·s^{-1}, and the vertical airflow creates a cyclone effect at TB2 (where the height of the cyclone center from the ground is 0.35 m, and the distance from the solid board in front of the pigpen is 2.5 m). The airflow trajectory in pigpen No.3 is analogous to that in pigpen No.2, with a mass flow rate of –0.003 kg·s^{-1} at the slatted floor.

(3) In pigpen No.6, the airflow converges with that of the manure pit, leading to the formation of a cyclone parallel to the ground at position TB3. Similarly, the airflow trajectory in pigpen No.5 mirrors that of pigpen No.6. At position MP4, the airflow diverges towards both sides; one portion flows towards the front of the piggery and ultimately enters pigpen No.1, while the other flows towards the rear and is expelled from the piggery via fans.

(4) In pigpen No.7, airflow beneath the slatted floor enters from the front of the pigpen, with part of it flowing into the upper airflow and the remainder re-entering the manure at the rear of the pigpen. The airflow trajectory in pigpen No.9 is akin to that in pigpen No.7.

(5) Influenced by the negative pressure fan, the airflow in pigpen No.10 predominantly moves towards the fan, with a mass flow rate of 0.062 kg·s^{-1} at the slatted floor. Notably, airflow within pigpens No.2 and No.10 is directed upward, whereas airflow in pigpens No.3 through No.9 is directed downward.

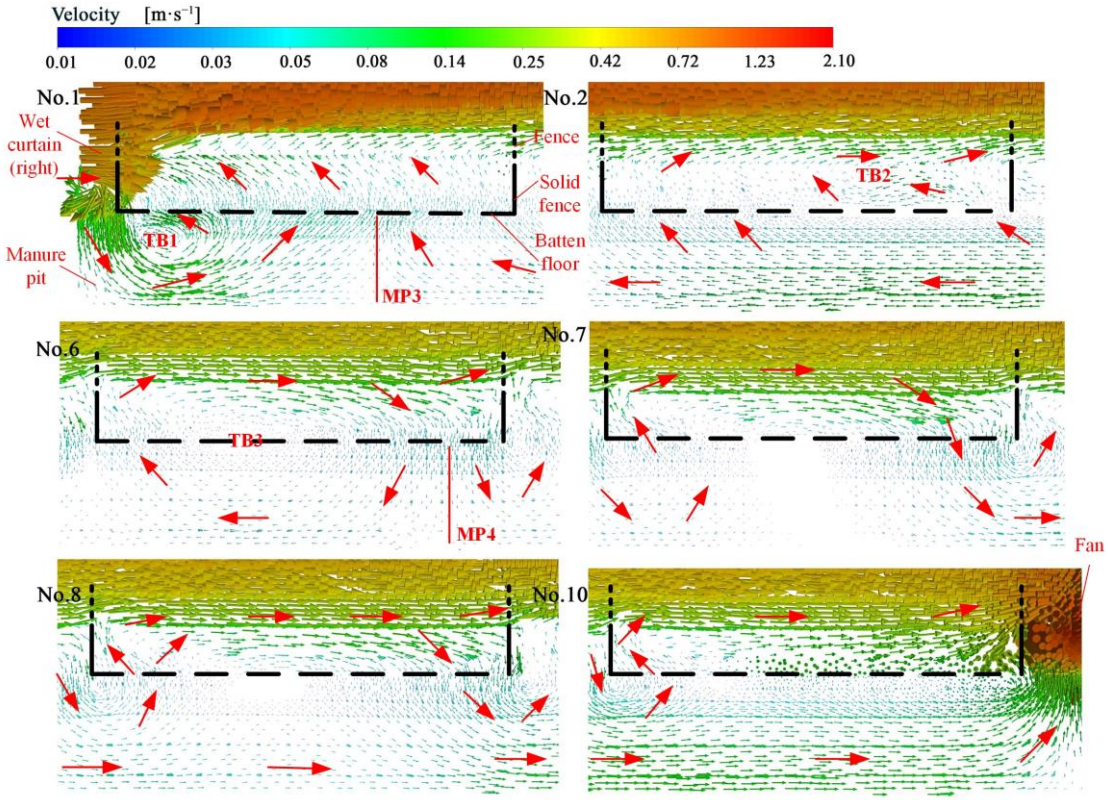

Fig. 6. Airflow trajectory on the *xz* surface of TB-type pigpen.

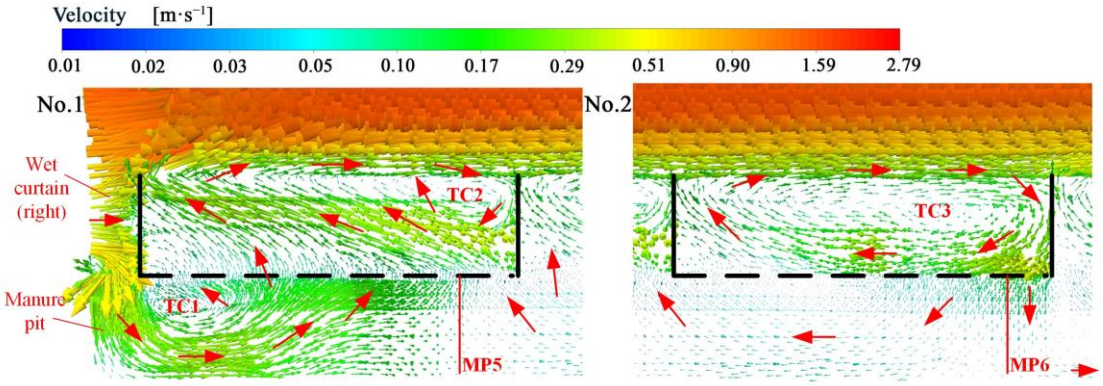

Fig. 7. Airflow trajectory on the *xz* surface of TC-type pigpen.

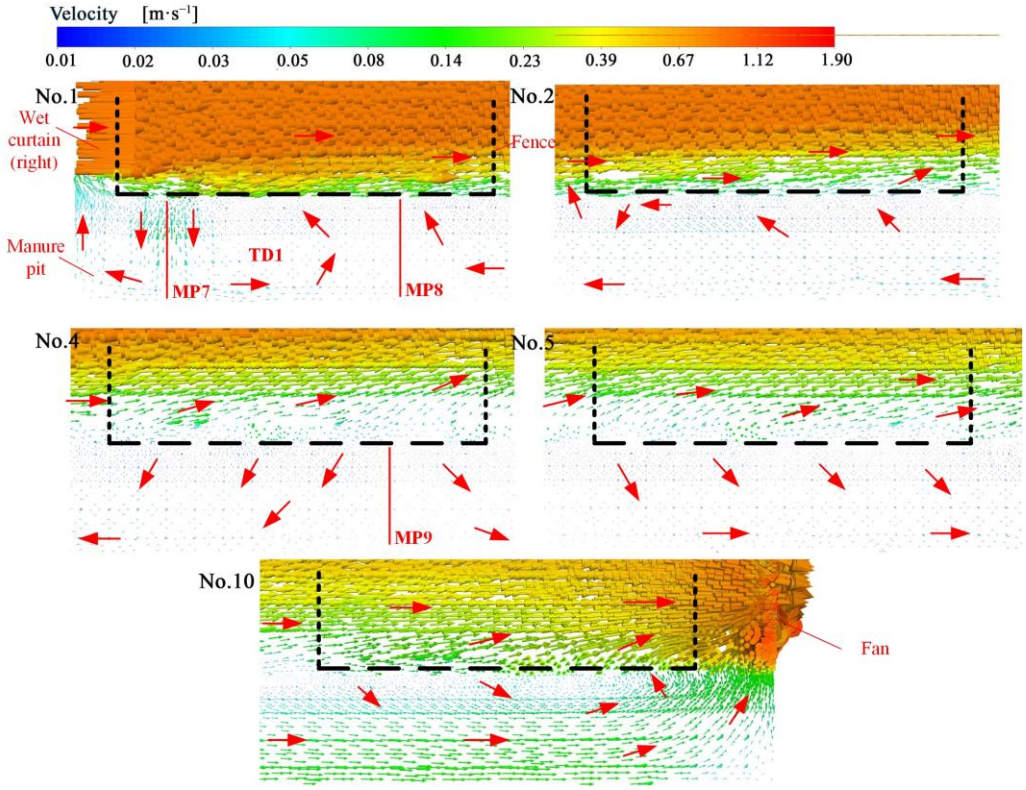

Fig. 8. Airflow trajectory on the *xz* surface of TD-type pigpen.

Analysis of Airflow Trajectory in TC Pigpen

The side of the TC pigpen near the aisle is fenced, while the other three directions are solid boards. The airflow trajectory on the *xz* surface of the pigpen is illustrated in Fig. 7. The height of the TC pigpen matches that of the TA, resulting in a similar upper airflow trajectory. Since the central aisle is fenced on both sides, air can flow freely to either side. Based on the airflow direction, the manure pit can be divided into three distinct areas. The horizontal distance from the front wall to position MP5 measures 3.9 m, which is 95% longer than that in the TA scheme and 30% longer than the TB scheme. A cyclone is located at TC1 within the manure pit, corresponding to the positions of TA1 and TB1. The distance between positions MP5 and MP6 is 3.8 m, which is 62% shorter than the TA scheme and 81.28% shorter than the TB scheme. Additionally, the horizontal distance from position MP6 to the front wall is 7.7 m, indicating a reduction of 38.83% compared to the TA scheme and 66.95% compared to the TB scheme.

When the airflow enters the manure pit, the distance to position MP5 is greater than that of both the TA and TB schemes. The comparative analysis is as follows:

(1) The mass flow rate of the airflow at the slatted floor in pigpen No.1 is 0.697 kg·s^{-1}, and its trajectory resembles that of the TA scheme.

(2) Similarly, the airflow trajectory and cyclone position in pigpen No.2 align with the TA scheme. At MP6, located beneath pigpen No.2, the airflow divides; part of it reverses direction, entering pigpen No.1 through the slatted floor, while the remaining portion flows towards the rear of the piggery.

(3) The airflow trajectories in pigpens No.3 to No.9 are consistent with those observed in pigpens No.4 to No.9 under the TA scheme. The airflow in the front pigpen traverses the slatted floor and enters the adjacent pigpen at the rear. In the TC scheme, the airflow in the manure pit exhibits a shorter retrograde distance.

Analysis of Airflow Trajectory in TD Pigpen

The TD pigpen is designed with fences that facilitate

unobstructed airflow. The airflow trajectory in the *xz* plane is illustrated in Fig. 8. Since the fence does not obstruct the flow of air, the airflow trajectory within the pigpen mirrors that of the upper layer. However, the airflow in the piggery diminishes gradually with increasing distance. Based on the direction of airflow, the manure pit can be categorized into four distinct areas; nevertheless, the airflow velocity in each area remains relatively low compared to other solutions. (1) The horizontal distance from the front wall to position MP7 is 1 m, and the airflow direction is reversed. The main reason for the formation of reverse airflow is that the airflow entering the piggery from the wet curtain is not blocked by the solid board in the aisle, so there is no downward airflow. (2) The horizontal distance from positions MP7 to MP8 is 2.2 m, and the airflow direction is forward. There is a cyclone at TD1, which is 1.9 m from the front wall of the piggery and 0.6 m from the ground surface. (3) The horizontal distance from positions MP8 to MP9 is 11.9 m, and the airflow direction is reversed. The horizontal distance between position MP9 and the back wall of the piggery is 24.9 m, and the airflow direction is positive. In the manure pit, the airflow between position MP9 and the front wall of the piggery will enter the pig activity area. (4) The horizontal distance between position MP9 and the front wall of the piggery is 15.1 m, which is 25.83%, –35.19%, and 96.1% farther away than the TA, TB, and TC schemes respectively. The comparative analysis is as follows:

(1) There are two airflow-dividing positions below pigpen No.1, namely MP7 and MP8. The mass flow rate of the airflow at the slatted floor in pigpen No.1 is –0.006 $kg \cdot s^{-1}$, and the airflow is divided at position MP7. Part of the airflow flows in the opposite direction and moves upward after being blocked by the front wall of the piggery; the other part of the airflow will form a cyclone at TD1 and enter the pigpen No.1 again.

(2) The airflow will be divided at MP9 below pigpen No.4, and the reverse airflow will eventually enter pigpens No.1 and No.2 through the slatted floor.

(3) In the TD scheme, the slatted floors of pigpens No.2 and No.10 are rising airflows with mass flow rates of 0.078 $kg \cdot s^{-1}$ and 0.177 $kg \cdot s^{-1}$ respectively, and the other pigpens are all downward airflows.

B. Analysis of the xy Plane Airflow Trajectory of the Pigpen

To enhance the study of airflow trajectories at the breathing height level of pigs, this research selected representative pigpens No.1, No.2, No.6, and No.10 from each analysis plan. The airflow trajectories in the *xy* plane (0.4 m from the ground). For each scheme is illustrated in Fig. 9.

The airflow trajectories in TA pigpens exhibits a similar pattern. At the height of the pig's breathing, the airflow is predominantly reversed, opposing the direction of the upper airflow. Pigpens No.1, No.2, and No.10 are situated relatively close to the air inlet and outlet, resulting in transverse airflow (in the *y*-axis direction) at the rear end of each pigpen. In contrast, pigpens No.3 through No.9 experience less disturbance, with the airflow speed at the front of the pigpen being greater than that at the back. Notably, there is no cyclone present in the breathing plane of pigs within TA pigpens.

In comparison to the TA pigpen, the solid board of the TB pigpen is lower and presents a limited obstruction to airflow. Changes in the airflow trajectory indicate that the wind speed in the pigpens located at the rear of the piggery is greater than that in the front pigpens. Notably, there is a reverse airflow in pigpen No.1, which shifts closer to the aisle during the flow process. The airflow in pigpens No.2 and No.3 is relatively complex, featuring reverse airflow near the aisle and positive airflow in other areas. In contrast, the airflow patterns in pigpens No.4 to No.10 are more uniform, predominantly exhibiting positive airflow.

TC pigpens are significantly influenced by aisle airflow. Each pigpen primarily exhibits reverse airflow, with a cyclone present in pigpens No.1 to No.4. As the distance of airflow travel increases, the cyclone speed in pigpens No.5 to No.10 diminishes. The airflow trajectory in the *xy* plane indicates that air enters from the rear of the pigpen, exits from the front, and subsequently flows into the middle aisle. The mass flow rates of the airflow at the fences of pigpens No.1, No.2, No.3, and No.10 are measured at 0.203 $kg \cdot s^{-1}$, 0.209 $kg \cdot s^{-1}$, 0.031 $kg \cdot s^{-1}$, and 0.019 $kg \cdot s^{-1}$, respectively (positive values indicate that the airflow direction is toward the positive *y*-axis), while the fences of the other pigpens exhibit negative airflow. Additionally, the fences on both sides of the aisle enhance ventilation efficiency within the pigpen.

The TD pigpen is constructed entirely of fences, which facilitates unrestricted airflow. At the breathing height of the pigs in TD pigpens, the airflow speed is relatively high and predominantly consists of positive airflow.

C. Analysis of Cloud Charts and Data

Analysis of Changes in Wind Speed

The wind speed cloud diagram at the breathing height of nursery pigs is illustrated in Fig. 10. The wind speed cloud chart intuitively shows that in schemes TA, TB, and TC, the high wind speed areas are primarily concentrated in the middle aisle, whereas in TD scheme, they are predominantly located at the front of the piggery. Table I indicates that under the same environmental conditions, the average wind speeds at the breathing height plane of pigs in TA, TB, TC, and TD type pigpens are 0.11 $m \cdot s^{-1}$, 0.15 $m \cdot s^{-1}$, 0.13 $m \cdot s^{-1}$, and 0.32 $m \cdot s^{-1}$, respectively. Among these, the TA scheme exhibits the lowest average wind speed, while the TD scheme demonstrates the highest average wind speed. The coefficients of variation of wind speed for the four schemes are 45.87%, 45.18%, 46.89%, and 48.42%, respectively. Notably, the TD scheme shows the greatest variation in wind speed, with values ranging from 0.05 to 0.78 $m \cdot s^{-1}$. Conversely, the TB scheme has the smallest variation, with wind speed values ranging from 0.04 to 0.41 $m \cdot s^{-1}$. This implies that the solid board effectively obstructs airflow, thereby better maintaining consistent airspeed within the pigpen. While the fence structure of the pigpen enhances the overall ventilation efficiency, it also contributes to increased variation in wind speed. Consequently, this variability may impede the precision of the environmental control system in large-scale operations.

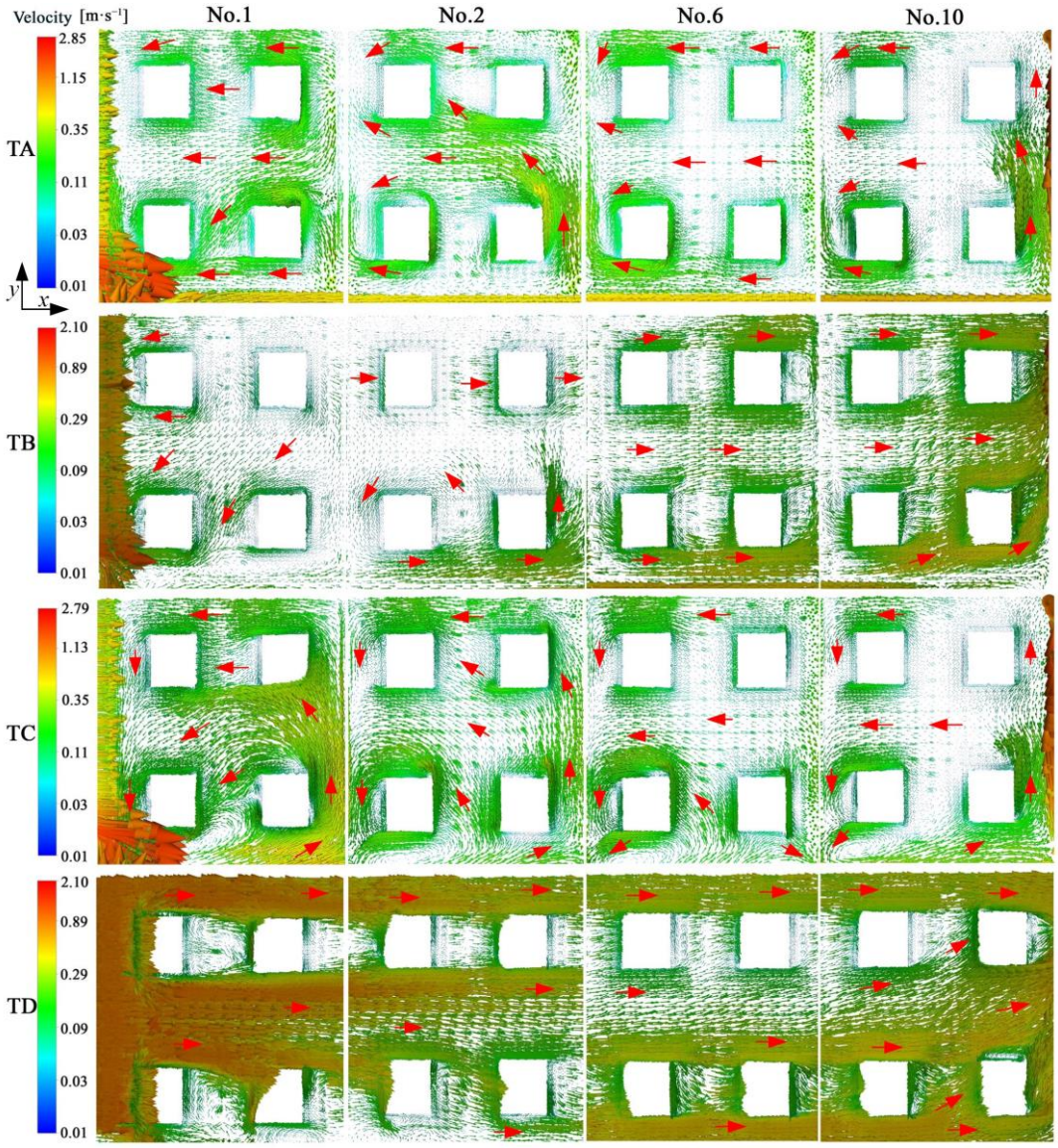

Fig. 9. Airflow trajectory of pig breathing plane.

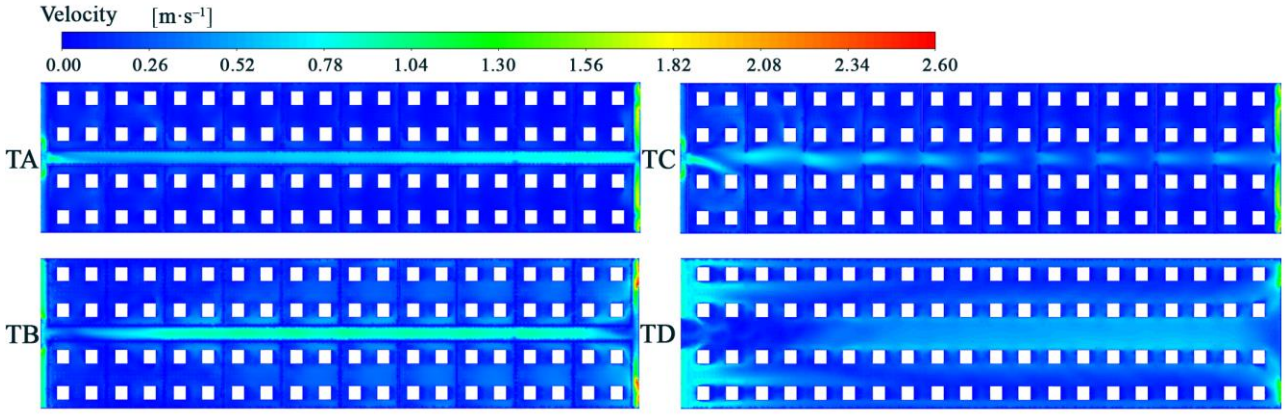

Fig. 10. Wind speed change chart.

TABLE I
COMPARATIVE ANALYSIS OF ENVIRONMENTAL VALUES AT MONITORING POINTS.

Type	Wind speed (m·s⁻¹)			Temperature (℃)			Average value		Coefficient of variation	
	Max	Min	Deviation	Max	Min	Deviation	Wind speed (m·s⁻¹)	Temperature (℃)	Wind speed	Temperature
TA	0.27	0.04	0.23	24.39	20.3	4.09	0.11	22.20	45.87%	3.3%
TB	0.41	0.04	0.37	24.65	20.3	4.35	0.15	22.48	45.18%	3.3%
TC	0.51	0.04	0.47	23.52	20.29	3.23	0.13	21.76	46.89%	2.71%
TD	0.78	0.05	0.73	23.94	20.04	3.9	0.32	21.87	48.42%	3.75%

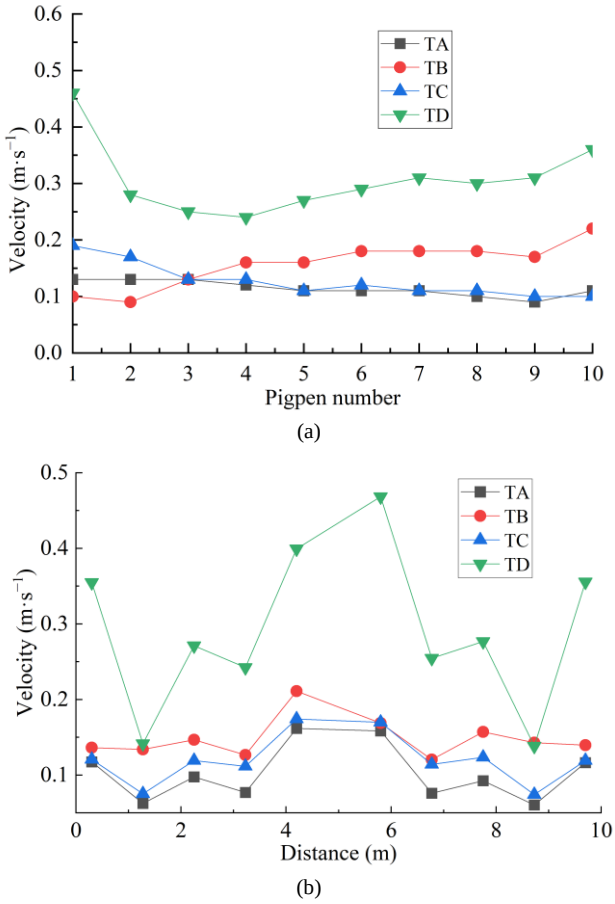

Fig. 11. Analysis of wind speed changes:(a) Comparison of average wind speed in the pigpen; (b) Comparison of average wind speeds on the left and right sides of the pigpen.

TABLE II
COMPARISON OF ENVIRONMENTAL DIFFERENCES AMONG VARIOUS SCHEMES

Type		Comparison of average values		*p*	
		Wind speed (m·s⁻¹)	Temperature (℃)	Wind speed	Temperature
TA−TB		−0.04	−0.28	0.00**	0.00**
TA−TC		−0.02	0.44	0.03*	0.00**
TA−TD		−0.21	0.33	0.00**	0.00**
TB−TC		0.03	0.72	0.00**	0.00**
TB−TD		−0.16	0.62	0.00**	0.00**
TC−TD		−0.19	−0.11	0.00**	0.09
TA	left−right	−0.00	0.01	0.79	0.94
TB		−0.00	0.01	0.68	0.89
TC		0.00	0.04	0.97	0.65
TD		0.02	0.08	0.10	0.35

* $p < 0.05$; ** $p < 0.01$

Fig. 11-a illustrates the average wind speed values for pigpens No.1 to No.10, while Fig. 11-b depicts the wind speed values on the left and right sides of the piggery, using the right wall as the reference point. As shown in Table II, significant differences in wind speed values exist among the various schemes ($p < 0.05$). The pigpens located at the front and rear of the piggery are influenced by the air inlet and air outlet, respectively. Notably, the average wind speed in the pigpen is higher than that in the central pigpen of the facility. In the TA and TC schemes, the solid board impeded the airflow, resulting in a gradual decrease in airflow speed. Conversely, in the TB and TC solutions, the solid board is lower, causing less obstruction to airflow and resulting in a progressive increase in airflow speed. The wind speed near the left and right walls of the piggery, as well as in the central aisle, is relatively higher. Among the various schemes, the wind speed in scheme TB is notably more stable.

Analysis of Temperature Changes

Temperature is a primary concern in the environmental regulation of piggery operations. By combining Fig. 12 and Fig. 13, it is evident that among the four options, the temperature in the pigpen located at the front of the piggery is significantly affected by the wet curtain and the manure pit, resulting in a lower temperature in this area compared to other pigpens. Under identical environmental conditions, the average temperatures for schemes TA, TB, TC, and TD are recorded as 22.20°C, 22.48°C, 21.76°C, and 21.87°C, respectively (As shown in Table I). Notably, except for the TC and TD schemes, there are extremely significant differences in temperature values between the schemes ($p < 0.01$). However, no significant differences in temperatures were detected on the left and right sides of the piggery across each scheme ($p < 0.05$), as illustrated in Table II. Among the four schemes, the TC scheme exhibits the lowest average temperature and the smallest temperature variation, with a range of 20.29°C to 23.52°C. The TB scheme demonstrates the best thermal insulation effect, with an average temperature that is 3.31% higher than that of the TC scheme. The coefficients of variation for temperature among the four schemes are 3.3%, 3.3%, 2.71%, and 3.75%, respectively. The TC scheme shows the least degree of dispersion in temperature values across various monitoring points, while the dispersion in the data for the TA and TB schemes is equivalent.

As illustrated in Fig. 13-a, the temperature variations in the rear pigpens of the TB and TD schemes are relatively stable, except for those pigpens located at the front. These front pigpens are significantly influenced by the temperature in the manure pit. In contrast, the TA and TC schemes demonstrate a gradual increase in average temperature within the piggery as the distance from the airflow source increases. This phenomenon can be attributed to the solid plate's relatively good thermal insulation performance. As the airflow progresses, the warm air gradually migrates towards the rear of the piggery. In the TB and TD schemes, the barriers to the airflow are less obstructive, resulting in smaller differences in average temperatures among the various pigpens. Fig. 13-b further illustrates that, across all schemes, the high-temperature zones are predominantly concentrated along both sides of the piggery.

IV. DISCUSSION

(1) Research findings

During the research process, the following main issues were discovered:

1) The solid board can effectively obstruct airflow parallel to the ground; however, as the height of the solid board increases, it becomes more likely to induce a cyclone effect within the pigpen, leading to the accumulation of airflow.

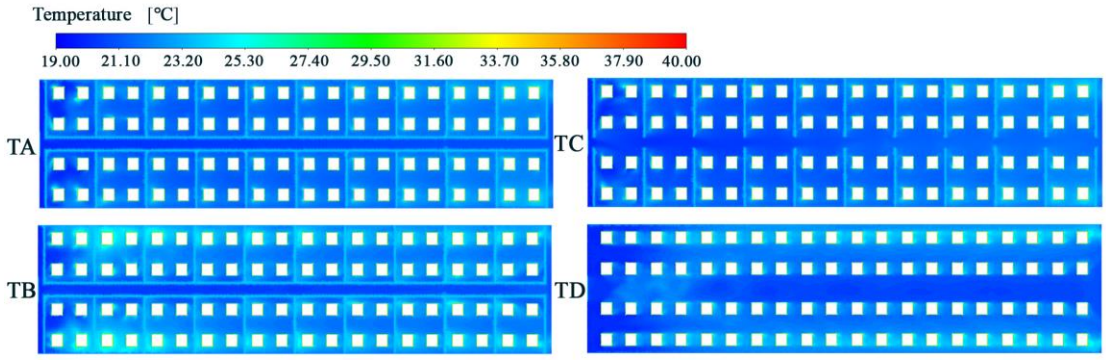

Fig. 12. Temperature change chart of the piggery.

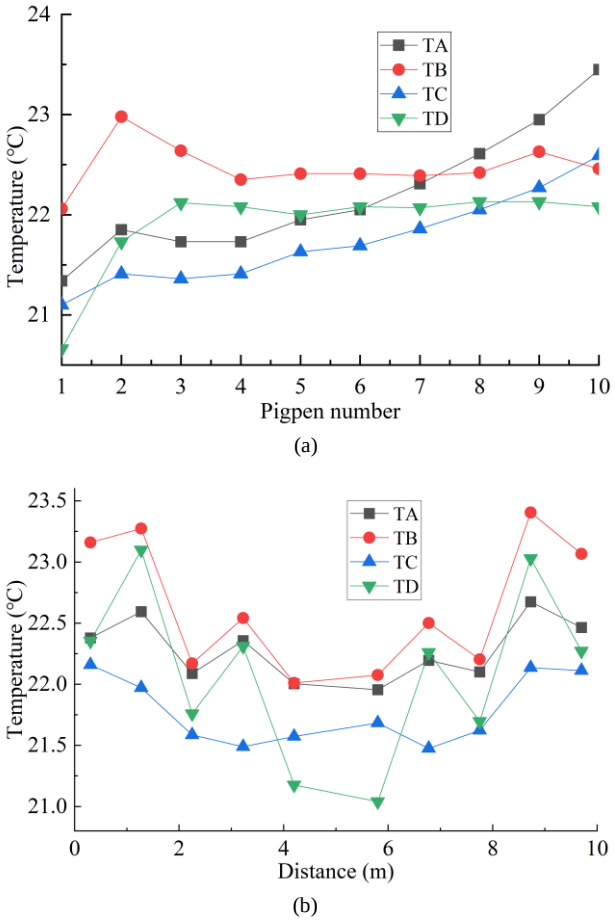

Fig. 13. Temperature change analysis:(a) Comparison of average temperature in the pigpen;(b) Comparison of average temperature on the left and right sides of the pigpen.

2) After the airflow passes through the wet curtain, it is obstructed by the solid board, causing the air to flow downward into the manure pit. The airflow entering the manure pit creates a cyclone at a specific position, which drives harmful gases from the manure pit back into the pigpen.

3) Reverse airflow can easily occur in the manure pit of a closed piggery, leading to the backflow of harmful gases. In subsequent research, measures should be implemented to prevent this backflow of harmful gases.

4) The proportion of solid boards in the pigpen significantly influences the changes in wind speed within the pigs' activity area. Replacing the solid boards on both sides of the middle aisle with fences can effectively lower the temperature at the pigs' breathing plane. Among the four schemes evaluated, the TC scheme exhibits the lowest temperature at the respiratory plane of the pigs, along with the lowest coefficient of temperature variation.

(2) The ideal pigpen

Utilizing CFD technology for airflow trajectory simulation analysis reveals that reverse airflow is a common occurrence across all examined schemes. The presence of reverse airflow not only prolongs the air replacement time within the piggery but also poses risks to the healthy growth of pigs. Consequently, further investigation into the pigpen structure is essential in subsequent research to mitigate the occurrence of reverse airflow.

(3) Error analysis of simulation results

This study thoroughly analyzes relevant cases to construct both a structural model and a simulation calculation model aimed at minimizing the error in simulation results. The literature indicates that, for current CFD simulations, the relative error in temperature can be maintained below 10%, while the wind speed error can be kept below 30%. The application of established computational models and methods ensures low simulation errors. Consequently, this study obviates the necessity of comparing simulation results with actual measured values, thereby significantly reducing the consumption of scientific research resources and time.

In this study, the temperature within the manure pit was not considered, which may result in lower temperatures in the pigpen at the front of the piggery. Simplifying the pig's form to a cube will influence the airflow trajectory across the pig's body surface, subsequently affecting the airflow trajectory at the respiratory level. The manure pits beneath the experimental piggeries are sealed; however, some piggeries feature ventilation openings that are not uniformly positioned. If vents are present in the manure pit, it is sufficient to incorporate additional vents into the model. Future research should concentrate on the ventilation openings of the manure pit to minimize the likelihood of airflow from the manure pit entering the pigpen.

(4) Innovation and advantages

Currently, the construction of piggeries is primarily based on experience and lacks a solid scientific foundation. This study employed CFD technology, using the pigpen as the research unit, to investigate the effects of different types of pigpens on airflow and temperature within the piggery. Scientific methods were utilized to elucidate the impact of various pigpen designs on airflow in piggeries. By simulating the piggery environment with CFD technology, the study

effectively illustrates the environmental changes that occur, significantly reducing the costs associated with scientific research. The findings of this research can serve as a valuable reference for piggery construction, and the methodologies, modeling techniques, and computational models developed during the experimental process can be applied to the

simulation analysis of different environmental scenarios, demonstrating substantial practical value.

(5) Application prospects

This study offers a comprehensive analysis of the influence of various types of pigpens on airflow within the piggery and the respiratory conditions of the pigs, thereby serving as a valuable reference for piggery construction. The simplified model, calculation model, simulation software, and research methodologies presented in this simulation approach can be effectively utilized for ventilation research across diverse application scenarios, significantly enhancing the efficiency of scientific inquiry. When confronted with different construction patterns in various application scenarios, only the boundary conditions and model structures need to be adjusted to fulfill the simulation requirements. Consequently, varying types of application scenarios can be examined consistently. In the context of closed piggeries, which are prevalent in Henan, rectangular closed piggeries are the most common. Throughout different seasons, the ventilation patterns within a closed piggery remain largely unchanged. During the subsequent construction phase of the piggery, only the model requires appropriate modifications to satisfy the simulation criteria. CFD technology has great application value in the study of piggery environments.

(6) Potential challenges

This method can be applied to a variety of scenarios in both agricultural and industrial fields. However, as the range of application scenarios expands and environmental variables increase, the computational burden on the computer also rises. The implementation of CFD technology and related software imposes higher demands on users, necessitating a greater level of professional knowledge and skills. As subsequent research progresses, the range of environmental variables under investigation will expand, leading to longer simulation calculation times, greater computational demands, and heightened requirements for computer configurations.

V. Conclusions

This study focuses on a longitudinally ventilated closed piggery as the research subject and employs CFD technology as the primary research method. It proposes a technical approach to analyze variations in temperature and airflow within the piggery. To accurately assess the influence of different pigpen types on the piggery environment, the study utilizes a widely recognized calculation model and constructs a structural model based on the actual design of the piggery. CFD technology is applied to evaluate the effects of four different fence types on the piggery environment under uniform environmental conditions. The main conclusions of this study are as follows:

(1) The four types of pigpen structures exhibit significant differences in their impact on the airflow trajectory within the piggery. In the TA scheme, a reverse airflow occurs in the breathing zone of the pigs, which adversely affects air quality improvement in the piggery. In the TB scheme, both positive and reverse airflows are present in pigpens No. 1 and No. 2, while positive air flow predominates in the remaining pigpens. In the TC scheme, airflow from the pigpen is directed towards the aisle located in the middle of the piggery, thereby enhancing overall air circulation. Finally, in the TD scheme, the airflow within the pigpen is predominantly positive.

(2) The four pigpen structures exhibit differing impacts on wind speed and temperature values within the piggery. Specifically, TA scheme records the lowest average wind speed, whereas TD scheme demonstrates the highest average wind speed. Additionally, the dispersion degree of wind speed in TD scheme is the largest, recorded at 48.42%, which may hinder the uniform adjustment of wind speed in the piggery during subsequent stages. In all schemes, the average temperature at the respiratory height plane of the pigs is approximately 22°C; however, the temperature values among the monitoring points in scheme TC show the least dispersion.

(3) The combined distribution structure of various types of pigpens will foster an optimal environment for pig farming. As demonstrated above, the TA scheme is more effective in reducing wind speed and retaining heat, whereas the TD scheme offers superior ventilation and cooling effects. The TC type pigpen incorporates the advantages of both the TA and TD schemes, thereby exhibiting the most significant benefits in the research. Consequently, in future research, these four types of pigpens can be strategically combined and arranged based on the evolving characteristics of the overall environment within the piggery. This approach aims to enhance the uniformity of environmental factor distribution in the piggery and mitigate the risk of local optimality.

In summary, CFD technology can be utilized to effectively construct a mathematical model of environmental factor distribution, thereby providing a scientific basis for the construction and selection of piggeries.

References

[1] Kim, J. G., Lee, I. B., Lee, S. Y., Park, S.J., Jeong, D. Y., Choi, Y. B., and Yeo, U. H., "Development of an air-recirculated ventilation system for a piglet house, part 1: Analysis of representative problems through field experiment and aerodynamic analysis using CFD simulation for evaluating applicability of system". Agriculture, vol. 12, no. 8, p. 1139, 2022.

[2] Oh, B. W., Seo, H. J., Seo, and I. H., "Ventilation Operating Standard for Improving Internal Environment in Pig House Grafting Working Conditions Using CFD". AgriEngineering, vol. 5, no. 3, pp. 1378-1394. 2023.

[3] Li, Y., Fu, C., Yang, H., Li, H., Zhang, R., Zhang, Y., and Wang, Z., "Design of a closed piggery environmental monitoring and control system based on a track inspection robot". Agriculture, vol. 13, no. 8, p. 1501, 2023.

[4] Shin, H., Kwak, Y., Jo, S. K., Kim, S. H., Huh, and J. H., "Development of an optimal mechanical ventilation system control strategy based on weather forecasting data for outdoor air cooling in livestock housing". Energy, vol. 268, p. 126649, 2023.

[5] Choi, Y. B., Kim, J. G., Cho, J. H., Lee, S. Y., Park, and S. J., "Estimation of ventilation rate in a piglet house considering ventilation system characteristics". Biosystems Engineering, vol. 227, pp. 1-18, 2023.

[6] Lee, S. Y., Choi, L. Y., Park, J., Daniel, K. F., Hong, S. W., Kwon, K., and Hwang, O., "Evaluation of Actual Ventilation Rates and Efficiency in Research-Scale Pig Houses Based on Ventilation Configurations". Animals, vol. 13, no. 15, p. 2451, 2023.

[7] Bai, Z. P., and Li, Y. F., "Effect of longitudinal ventilation on smoke temperature below utility tunnel ceiling". Engineering Letters, vol. 28, no. 3, pp. 939-943, 2020.
[8] Hansen, M. J., Guldberg, L. B., and Feilberg, A., "Effect of slurry funnels with partial pit ventilation on emissions from pig houses". Biosystems Engineering, vol. 229, pp. 200-208, 2023.
[9] Yeo, U. H., Lee, I. B., Kim, R. W., Lee, S. Y., Kim, and J. G., "Computational fluid dynamics evaluation of pig house ventilation systems for improving the internal rearing environment". Biosystems Engineering, vol. 186, pp. 259-278, 2019.
[10] Rong, L., Bjerg, B., and Zhang, G., "Assessment of modeling slatted floor as porous medium for prediction of ammonia emissions–Scaled pig barns". Computers and Electronics in Agriculture, vol. 117, pp. 234-244, 2015.
[11] Gao, L., Er, M., Li, L., Wen, P., Jia, Y., and Huo, L., "Microclimate environment model construction and control strategy of enclosed laying brooder house". Poultry Science, vol. 101, no.6, p. 101843, 2022.
[12] Hou, F., Shen, C., and Cheng, Q., "Research on a new optimization method for airflow organization in breeding air conditioning with perforated ceiling ventilation". Energy, vol. 254, p. 124279, 2022.
[13] Küçüktopcu, E., Cemek, B., Simsek, H., Ni, and J. Q., "Computational fluid dynamics modeling of a broiler house microclimate in summer and winter". Animals-Basel, vol. 12, p. 867, 2022.
[14] Xin, Y, Rong, L., Wang, C., Li, B., and Liu, D., "CFD study on the impacts of geometric models of lying pigs on resistance coefficients for porous media modelling of the animal occupied zone". Biosystems engineering, vol. 222, pp. 93-105, 2022.
[15] Bai, Z. B., Zhao, X. H., Song, H. T., Qin, H.J., Zhang, Y., and Yao, H.W., "Numerical simulation study on ventilation effect in utility tunnel". Engineering Letters, vol. 32, no.6, pp. 1090-1096, 2024.
[16] Son, H., Lee, S., Um, J., and Lee, S., "Analysis of Ventilation Performance in Pig Houses using CFD of Multi-Species Transport". Journal of the Wind Engineering Institute of Korea, vol. 23, no. 4, pp. 181-187, 2019.
[17] Wei, X., Li, B., Lu, H., Lü, E., Guo, J., Jiang, Y., and Zeng, Z., "Numerical Simulation of Airflow Distribution in a Pregnant Sow Piggery with Centralized Ventilation". Applied Sciences, vol. 12, no. 22, p. 11556, 2022.
[18] Mossad, R. R., "Optimization of the ventilation system for a forced ventilation piggery". Journal of Green Building, vol. 4, no. 4, pp. 113-133, 2009.
[19] Yang, H., Li, Y., Fu, C., Zhang, R., Li, H., Feng, Y., and Nie, F., "Research on inspection route of hanging environmental robot based on computational fluid dynamics". Journal of Agricultural Engineering, vol. 55, no.2, p. 1565, 2024.
[20] La, A., Zhang, Q., and Cicek, N., "Modelling aerosol transmission of porcine reproductive and respiratory syndrome virus between buildings using computational fluid dynamics". Biosystems Engineering, vol. 236, pp. 175-192, 2023.
[21] Tabase, R. K., Bagci, O., De Paepe, M., Aarnink, A. J., and Demeyer, P., "CFD simulation of airflows and ammonia emissions in a pig compartment with underfloor air distribution system: Model validation at different ventilation rates". Computers and electronics in agriculture, vol. 171, p. 105297, 2020.
[22] Yeo, U. H., Decano-Valentin, C., Ha, T., Lee, I. B., Kim, R. W., Lee, S. Y., and Kim, J. G., "Impact analysis of environmental conditions on odour dispersion emitted from pig house with complex terrain using CFD". Agronomy, vol. 10, no. 11, p. 1828, 2020.
[23] Saha, C. K., Yi, Q., Janke, D., Hempel, S., Amon, B., and Amon, T., "Opening size effects on airflow pattern and airflow rate of a naturally ventilated dairy building—A CFD study. Appl". Applied Sciences, vol. 10, no. 17, p. 6054, 2020.
[24] Tomasello, N., Valenti, F., Cascone, G., and Porto, S. M., "Development of a CFD model to simulate natural ventilation in a semi-open free-stall barn for dairy cows". Buildings, vol. 9, no. 8, p. 183, 2019.
[25] Li, H., Rong, L., and Zhang, G., "Reliability of turbulence models and mesh types for CFD simulations of a mechanically ventilated pig house containing animals". Biosystems Engineering, vol. 161, pp. 37-52, 2017.
[26] Wang, X., Zhang, G., and Choi, C. Y., "Effect of airflow speed and direction on convective heat transfer of standing and reclining cows". Biosystems Engineering, vol. 167, pp. 87-98, 2018.
[27] Mondaca, M. R., Choi, C. Y., and Cook, N. B., "Understanding microenvironments within tunnel-ventilated dairy cow freestall facilities: Examination using computational fluid dynamics and experimental validation". Biosystems Engineering, vol. 183, pp. 70-84, 2019.
[28] Kibwika, A. K., Seo, H. J., and Seo, I. H., "CFD model verification and aerodynamic analysis in large-scaled venlo greenhouse for tomato cultivation". AgriEngineering, vol. 5, no.3, pp. 1395-1414, 2023.
[29] Lin, J., Liu, J., Meng, Q., Lei, M., Tong, Y., and Gao, Y., "Numerical CFD simulation and verification of summer indoor temperature and airflow field in boar building". Transactions of the Chinese Society of Agricultural Engineering, vol. 32, no.23, pp. 207-212, 2016.
[30] Jung, S., Chung, H., Mondaca, M. R., Nordlund, K. V., and Choi, C. Y., "Using computational fluid dynamics to develop positive-pressure precision ventilation systems for large-scale dairy houses". Biosystems Engineering, vol. 227, pp. 182-194, 2023.
[31] Pakari, A., and Ghani, S., "Comparison of different mechanical ventilation systems for dairy cow barns: CFD simulations and field measurements". Computers and Electronics in Agriculture, vol. 186, p. 106207, 2021.
[32] Bournet, P. E., and Rojano, F., "Advances of Computational Fluid Dynamics (CFD) applications in agricultural building modelling: Research, applications and challenges". Computers and Electronics in Agriculture, vol. 201, p. 107277, 2022.
[33] Rong, L., Nielsen, P. V., Bjerg, B., and Zhang, G., "Summary of best guidelines and validation of CFD modeling in livestock buildings to ensure prediction quality". Computers and Electronics in Agriculture, vol. 121, pp. 180-190, 2016.
[34] Fang, J., Wu, S., Wu, Z., and Ba, W., "CFD simulation of vertical ventilation in nursery pig house and optimization design of windshield". Journal of Northeast Agriultural University, vol. 53, no. 5, pp. 59-68, 2022.
[35] Qi, F., Zhao, X., Shi, Z., Rong, L., Zhang, G., and Li, H., "Applicability evaluation of innovative simplified methods of slatted floor in pig houses–A CFD study". Computers and Electronics in Agriculture, vol. 216, p. 108532, 2024.
[36] Drewry, J. L., Mondaca, M. R., Luck, B. D., and Choi, C. Y., "A computational fluid dynamics model of biological heat and gas generation in a dairy holding area". Transactions of the ASABE, vol. 61, no. 2, pp. 449-460, 2018.
[37] Gautam, K. R., Rong, L., Iqbal, A., and Zhang, G., "Full-scale CFD simulation of commercial pig building and comparison with porous media approximation of animal occupied zone". Computers and Electronics in Agriculture, vol. 186, p. 106206, 2021.
[38] Cano, D. V., Flores-Velazquez, J., and Garcia, A. R., "Natural Ventilation to Manage Ammonia Concentration and Temperature in a Rabbit Barn in Central Mexico". Applied Sciences, vol. 14, no. 9, p. 3767, 2024.

Chengguo Fu is an associate professor of the School of Mechanical Engineering, Guizhou University of Engineering Science, and School of Mechanical and Electrical Engineering, Henan Institute of Science and Technology, China. His research interests include control algorithms, environmental engineering, equipment design, and fluid dynamics.

Yuhao Li is a PhD candidate of the College of Engineering, South China Agricultural University, China. His research interests include control algorithms, robotics development, equipment design, and fluid dynamics.